

Brain Microstructural White and Gray Matter Alterations after Cardiopulmonary Bypass: Anatomical Distribution and Corresponding Neurocognitive Deficit

Dan Abrahamov^{1*}, Oren Lev Ran¹, Efrat Sasson², Sharon Naparstek¹, Mordechai Salti¹, Mahmoud Abu Salah¹, Reut Hizkiya¹, Yaron Ishay¹, Evgeny Brotfine¹, Gideon Sahar¹ and Yael Refaely¹

¹The Department of Cardiothoracic Surgery, Soroka University Medical Center, Beer-Sheva, Israel

²WiselImage - Medical Imaging Services, Hod Hasharon, Israel

Abstract

Background: We sought to detect microstructural brain injury after coronary artery bypass grafting (CABG) using cardiopulmonary bypass (CPB) and to define its anatomical distribution. Analyses were performed to determine possible correlation with postoperative neurocognitive deficit.

Methods: Seven patients undergoing CPB-CABG were assigned for serial cerebral designated diffusion tensor (DTI)-magnetic resonance imaging (MRI) examinations, preoperatively, on postoperative day (POD) 1 and 5. Levels of mean diffusivity (MD) and fractional anisotropy (FA) were analysed to assess gray and white matter injury. BBB-disruption and microembolic load were concomitantly evaluated by dynamic contrast enhancement (DCE)-MRI and diffusion-weighted imaging (DWI)-MRI methods, respectively. Neuropsychological tests were performed one day preoperatively and on POD 5.

Results: Increase in MD and decrease in FA were evident on POD 1 in gray matter structures including the hippocampus (MD, 0.000768 mm²/s ± 0.0000347 versus 0.000804 mm²/s ± 0.0000267, p<0.01; FA, 0.180 ± 0.03 mm²/s versus 0.163 mm²/s ± 0.032, p<0.01), middle frontal gyrus (MD, 0.000989 mm²/s ± 0.0000487 versus 0.001068 mm²/s ± 0.0000553, p<0.01), orbital gyrus (MD, 0.000867 mm²/s ± 0.0000374 versus 0.000908 mm²/s ± 0.0000356, p<0.01) and in the following white matter structures: Superior longitudinal fasciculus (MD, 0.000836 mm²/s ± 0.0000384 versus 0.000874 mm²/s ± 0.0000359, p<0.01; FA, 0.324 mm²/s ± 0.018 versus 0.305 mm²/s ± 0.022, p<0.01), frontal white matter (FA, 0.277 mm²/s ± 0.031 versus 0.26 mm²/s ± 0.033, p<0.01) internal capsule (MD, 0.000772 mm²/s ± 0.0000648 versus 0.000803 mm²/s ± 0.0000601, p<0.01; FA, 0.364 mm²/s ± 0.032 versus 0.343 mm²/s ± 0.029, p<0.01) and corticospinal tract (MD, 0.000759 mm²/s ± 0.0000557 versus 0.00078 mm²/s ± 0.0000591, p<0.01; FA, 0.440 mm²/s ± 0.023 versus 0.411 mm²/s ± 0.023, p<0.01). Corticospinal tract fibre tracing showed significant decrease in postoperative fibre number. DTI findings persisted through POD 5 without spontaneous regression. BBB-disruption reflected by increased K^{trans} was detected in five patients (71%) on POD 1, mainly in frontal lobes and spontaneously restored by POD 5. Postoperative global cognitive score was reduced in all patients (98.2 ± 12 vs. 95.1 ± 11, p=0.032), predominantly in executive function and attention (91.8 ± 13 vs. 86.9 ± 12, p=0.042). Postoperative FA decline significantly correlated with delta K^{trans} (R=0.6) and with postoperative decline in attention and Go-no-Go response inhibition tests (R=0.66 and 0.63, respectively).

Conclusion: CABG using CPB elicits gray and white matter microstructure injury in the above-mentioned anatomical distribution. These alterations are associated with transient BBB-disruption and may account for postoperative neurocognitive dysfunction.

Abbreviations: BBB: Blood brain barrier; CABG: Coronary artery bypass grafting; CPB: Cardiopulmonary bypass; CST: Cortico-spinal tract; DCE-MRI: Dynamic contrast enhancement MRI; DLPFC: Dorsolateral prefrontal cortex; DTI- MRI: Diffusion tensor imaging MRI; DWI- MRI: Diffusion-weighted imaging MRI; FA: Fractional anisotropy; MD: Mean diffusivity; MRI: Magnetic resonance imaging; POD: Postoperative day; ROI: Region of interest; SLF: Superior longitudinal fasciculus

Keywords: Magnetic resonance imaging; Diffusion tensor imaging; Cardiopulmonary bypass; Neuropsychological test; Cognition

Introduction

The incidence of neurocognitive dysfunction after cardiac surgery using cardiopulmonary bypass (CPB) ranges between 18% and 48% [1-3]. Postoperative neuropsychological tests display characteristic impairment mainly in executive functions, attention and mental processing speed [3]. Although several mechanisms have been proposed including microembolization, regional cerebral hypoperfusion and inflammation [4,5], the primary causative mechanism remains unknown

and specific areas of brain injury have not been anatomically localized. We have recently shown that blood brain barrier (BBB)-disruption may occur after coronary artery bypass grafting (CABG) using CPB and may play a role in postoperative neurocognitive dysfunction, possibly by exposing brain tissue to inflammatory substances otherwise hindered [6]. In this aforementioned study, using designated dynamic contrast

***Corresponding author:** Dan Abrahamov, Department of Cardiac Surgery, Soroka Medical Centre, Beer Sheva, Israel, Tel: +972-6400-962; E-mail: danab3@clalit.org.il

Received December 06, 2017; **Accepted** December 14, 2017; **Published** December 21, 2017

Citation: Abrahamov D, Ran OL, Sasson E, Naparstek S, Salti M, et al. (2017) Brain Microstructural White and Gray Matter Alterations after Cardiopulmonary Bypass: Anatomical Distribution and Corresponding Neurocognitive Deficit. J Alzheimers Dis Parkinsonism 7: 409. doi: 10.4172/2161-0460.1000409

Copyright: © 2017 Abrahamov D, et al. This is an open-access article distributed under the terms of the Creative Commons Attribution License, which permits unrestricted use, distribution, and reproduction in any medium, provided the original author and source are credited.

enhancement (DCE) magnetic resonance imaging (MRI), transient BBB-disruption was detected in most patients, most prominent in frontal cerebral lobes, evident on postoperative day (POD) 1 and restored spontaneously by POD 5 [6]. Statistical correlation was established between BBB-disruption and postoperative neurocognitive deterioration [6].

Standard neuroimaging modalities may lack the resolution to identify subtle anatomical alterations and evidence of microstructural tissue injury after CABG. Diffusion tensor imaging (DTI) is a novel MRI technique that may be used to portray a map of the brain neural tracts (tractography) and enable investigation of selected tracts. This modality uses water molecules diffusion measured in six non-collinear directions to provide a three dimensional representation of water motion in the tissue and reveals details about microscopic tissue architecture [7,8].

The primary goal of this study was to assess white and gray matter integrity after CPB-CABG using DTI-MRI and to define the anatomical distribution of microstructural injury. Secondary goals were to determine whether there is a correlation between microstructural white and gray matter injury, represented by DTI indices, BBB-disruption and postoperative neurocognitive deficit.

Patients and Methods

Patient population

Seven consecutive patients referred for elective, first-time, isolated CABG using CPB were assigned to undergo serial designated MRI examinations. Patients were excluded from this study if age was 70 years or older, had a contraindication to undergo MRI examination or co-existing peripheral arterial disease, history of cerebrovascular disease, history of dementia, cognitive dysfunction or psychiatric disorder, uncontrolled diabetes mellitus or renal dysfunction defined as serum creatinine level above 1.8 mg/dL.

Study protocol

Each patient enrolled underwent three designated MRI examinations. Baseline MRI was performed one day prior to the operation; postoperative MRI examinations were performed on postoperative day (POD) 1 and 5. The MRI studies were analysed for microstructural brain tissue injury, BBB-disruption and for signs for microemboli using DTI-MRI, DCE-MRI and diffusion-weighted imaging (DWI)-MRI, respectively. The yield of these modalities has been previously detailed [7-10]. Neuropsychological tests were undertaken one day preoperatively (baseline) and on POD 5.

MRI scans protocol and analysis

MRI scan was performed on a 3T MRI system (Ingenia, Philips Inc, The Netherlands) using the following sequences: Anatomical images including T2 weighted imaging, FLAIR and 3D high resolution T1.

Dynamic contrast enhanced MRI (DCE-MRI) was performed using five T1 weighted Fast Low Angle Shot (FLASH) volumes with different flip angles (for calculation of T1 map) followed by 100 dynamic T1 weighted FLASH volumes with flip angle of 20 degrees. Bolus injection of Gd-DTPA was performed following seven volumes. Sequence parameters: For the T1 maps, TR=10 ms, TE 2.085ms, flip angles: 5, 10, 15, 20, 25, 30 degrees. For the dynamic scans: TR=3.92 ms, TE=2 ms, flip angle=20 degrees.

Diffusion tensor imaging MRI (DTI-MRI) was performed using echo planar imaging (EPI) sequence with 31 directions (including 2

b0 volumes). TR=9000 ms, TE=106 ms, FOV=22.4 cm, in plain spatial resolution: 1.75X1.75 mm², matrix: 128x128, 60 axial slices, slice thickness 2 mm.

All MRI scan analysis was performed by "WiseImage- Medical Imaging Services, Hod Hasharon, Israel".

DWI MRI analysis

Diffusion-weighted imaging (DWI) evaluation was performed based on the mean DWI volumes in the DTI sequence. A lesion was defined as high signal intensity on DWI as well as low signal in apparent diffusion coefficient (ADC) image. The lesions were counted for each scan (seven patients, three time points).

DTI image analysis

DTI image analysis was performed using the Explore-DTI software (Leemans et al., 2009). Mean diffusivity (MD) and fractional anisotropy (FA) values were measured and analysed.

Voxel Based Statistical analysis

Spatial normalization and statistical analysis were performed using the SPM software (version 12, UCL, London, UK). Spatial normalization was performed for each patient based on the mean DWI image with similar contrast to the template used in SPM (ICBM template, based on T1 contrast). The normalization parameters were applied on the DTI maps. Spatial smoothing with kernel size of 8 mm full width at half maximum (FWHM) was applied.

Paired t-test was performed using voxel-based analysis, comparing pre- and postoperative results (POD 1 and POD 5, each compared to preoperative results) generating statistical parametric maps. The statistical parametric maps (p values) are presented superimposed on a T1 image from a single subject to permit informative anatomical reference. Using the statistical parametric maps for each of the statistical paired t-tests, significant voxels (p<0.001) were highlighted.

Values were extracted in significant clusters and mean \pm standard deviation of each time point were presented in graphs.

Correlations between mean MD and FA values and neuropsychological measures, as well as between average change in MD and FA values and average change in K^{trans} values were performed using the product-moment correlation module.

DTI Fibre tracking

Fibre tracking was applied using the ExploreDTI software. The principal eigenvectors and FA were used to generate the fibre coordinates, terminating at voxels with FA lower than 0.2 or following tract orientation change higher than 30°. Fibres that passed through a manually chosen seed region of interest (ROI) were plotted. The fibres were plotted as streamlines. Two fibre tracts were reconstructed: Cortico-spinal tract (CST) and superior longitudinal fasciculus (SLF).

CST was reconstructed using seed region of interest (ROI) in axial slices in the cortex and "END" ROI in the internal capsule. Where necessary, in order to eliminate fibres which are not part of the CST, a "no-fiber" plane was drawn in a coronal plane posterior to the CST (in the cerebellum) and in a sagittal plane eliminating fibers crossing to the contralateral hemisphere.

The SLF: Two ROIs were used to reconstruct the SLF. First ROI was drawn in a sagittal plane in the fronto-parietal part of the SLF and a second ROI was drawn in the parieto-temporal part of the SLF.

DCE MRI analysis

Images were corrected for motion using SPM software (version 12, UCL, London, UK). In short, T1 map was calculated and MR signal intensity of the dynamic scans was converted to Gd concentration. Arterial input function was calculated from the blood signal, the extended tofts pharmacokinetic model was applied and K_{trans}, V_e (extracellular-extravascular volume) and V_p (plasma volume) were calculated on a voxel by voxel basis. Smoothing of 4 mm FWHM was performed on the DCE maps.

DCE analysis was performed using in-house software written in Matlab as described previously (Roberts et al. 2006, Tofts, 1991, Tofts and Kermode, 1997, Tofts et al., 1999, Tofts, 2003).

Calculation of native T1 (T10): From the three flip angle images we acquire T10- native T1 (before injection) and S10.

Average DCE maps

Stripping of head from brain was performed using brain extraction tool. DCE images before and after surgery was spatial normalized by using the SPM software (version 12, UCL, London, UK). Spatial normalization was performed for each patient based on the first dynamic image to the ICBM template, based on T1 contrast. The normalization parameters were applied on the DCE maps. Spatial smoothing with kernel size of 4 mm full width half maximum (FWHM) was applied. An average K^{trans} map was calculated in each time point (pre-surgery, POD1 and POD5).

Neuropsychological tests

The Mindstreams[®] Cognitive Health Assessment (NeuroTrax[®] Corp) Computerized testing for cognitive functions system was used. Tests were age/education standardized. Tests were undertaken one day preoperatively and on POD 5 and included the following subtests: Go no go response inhibition. Cognitive domains evaluated: Attention, executive function.

Immediate and delayed verbal memory. Cognitive Domains evaluated: Immediate recognition memory, delayed recognition memory, Nonverbal memory. Stroop interference test. Cognitive domains evaluated: Attention, executive function.

The Global Cognitive Function score was computed as the average of the index scores.

Results

Mean age was 58 ± 10.9 years. Five patients (71%) were men. The mean CPB and cross-clamp time was 95.7 ± 37 (range, 48-148) and 83 ± 36.3 (range, 37-138) min, respectively. Grafts-patient ratio was 3.6 ± 0.8 (range 3-5).

There was no early mortality, major neurologic events or perioperative myocardial infarction. All preoperative MRI studies were examined by a roentgenologist and interpreted as normal.

POD 1 MRI was performed at mean 22 ± 3 h (range, 19-25) after the operation and at mean 13 ± 2 h (range, 11-15) after tracheal extubation. All patients were extubated and hemodynamically stable during the transport and MRI examination. The second postoperative MRI and second neuropsychological examination were performed on POD 5 in all patients. Patients did not receive analgesics or sedation one hour prior to or during the examination. All patients were discharged on POD 6.

Increase in mean diffusivity (MD) and decrease in fractional anisotropy (FA) were documented on POD 1 in gray matter structures: Hippocampus (MD 0.000768 mm²/s ± 0.0000347 versus 0.000804 mm²/s ± 0.0000267, p<0.01, FA 0.180 mm²/s ± 0.03 versus 0.163 mm²/s ± 0.032, p<0.01), Middle frontal gyrus (MD 0.000989 mm²/s ± 0.0000487 versus 0.001068 mm²/s ± 0.0000553, p<0.01), orbital gyrus (MD 0.000867 mm²/s ± 0.0000374 versus 0.000908 mm²/s ± 0.0000356, p<0.01) and in white matter structures: Superior longitudinal fasciculus (MD 0.000836 mm²/s ± 0.0000384 versus 0.000874 mm²/s ± 0.0000359, p<0.01, FA-0.324 mm²/s ± 0.018 versus 0.305 mm²/s ± 0.022, p<0.01), frontal white matter (FA 0.277 mm²/s ± 0.031 versus 0.26 mm²/s ± 0.033, p<0.01) internal capsule (MD 0.000772 mm²/s ± 0.0000648 versus 0.000803 mm²/s ± 0.0000601, p<0.01, FA 0.364 mm²/s ± 0.032 versus 0.343 mm²/s ± 0.029, p<0.01) and corticospinal tract (MD 0.000759 mm²/s ± 0.0000557 versus 0.00078 mm²/s ± 0.0000591, p<0.01, FA 0.440 mm²/s ± 0.023 versus 0.411 mm²/s ± 0.023, p<0.01) (Figures 1-3).

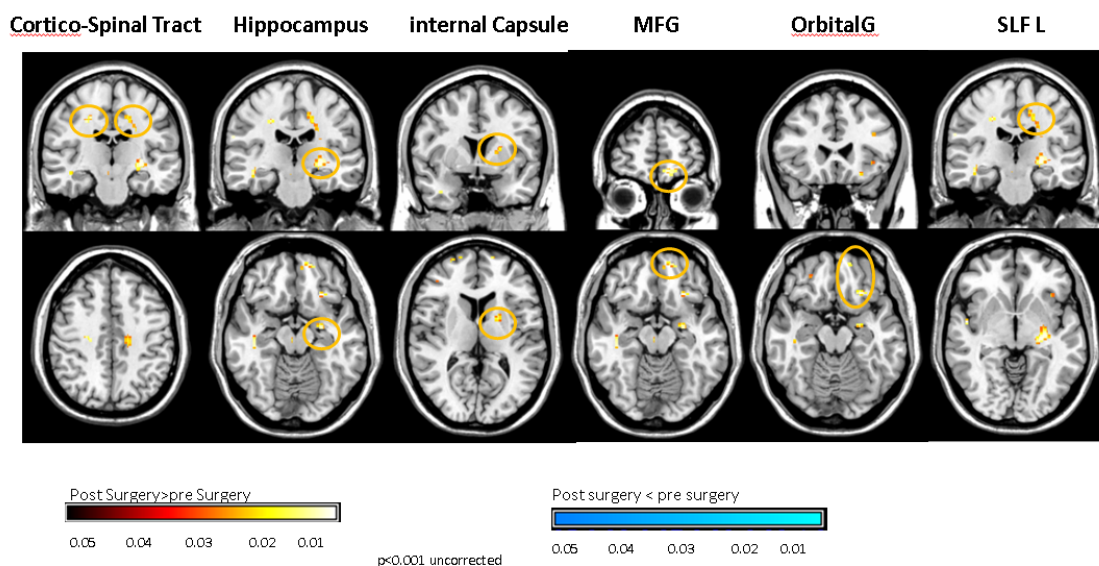


Figure 1: Change in mean diffusivity (MD). Postoperative day 1 compared to preoperative baseline.

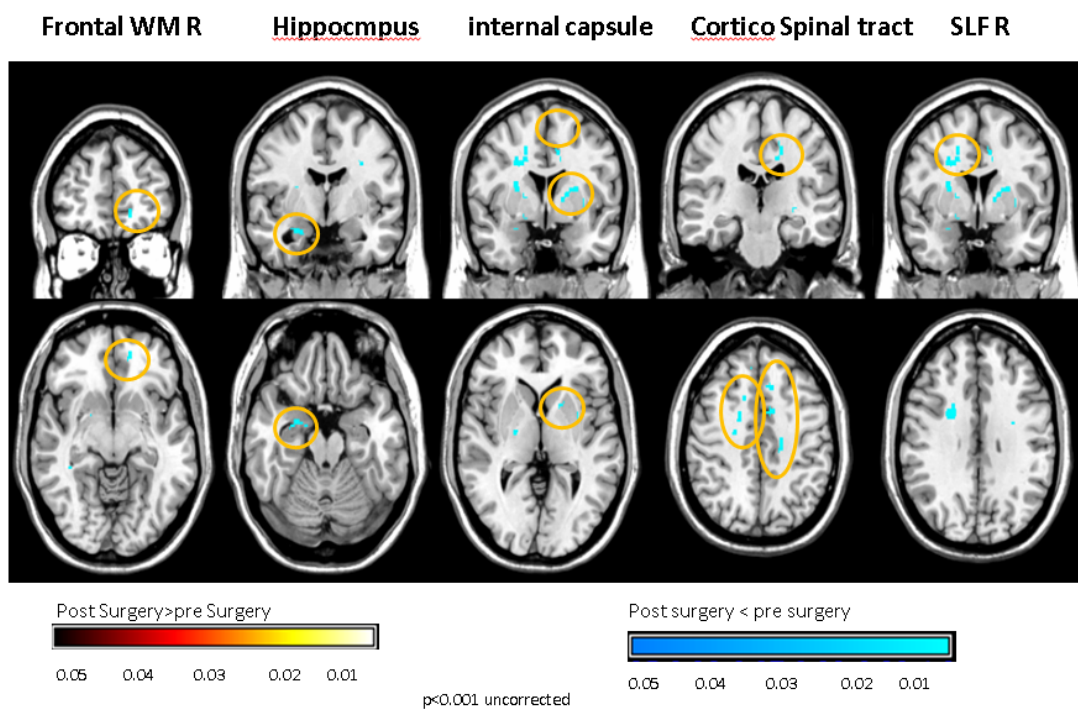


Figure 2: Change in fractional anisotropy (FA). Postoperative day 1 compared to preoperative baseline.

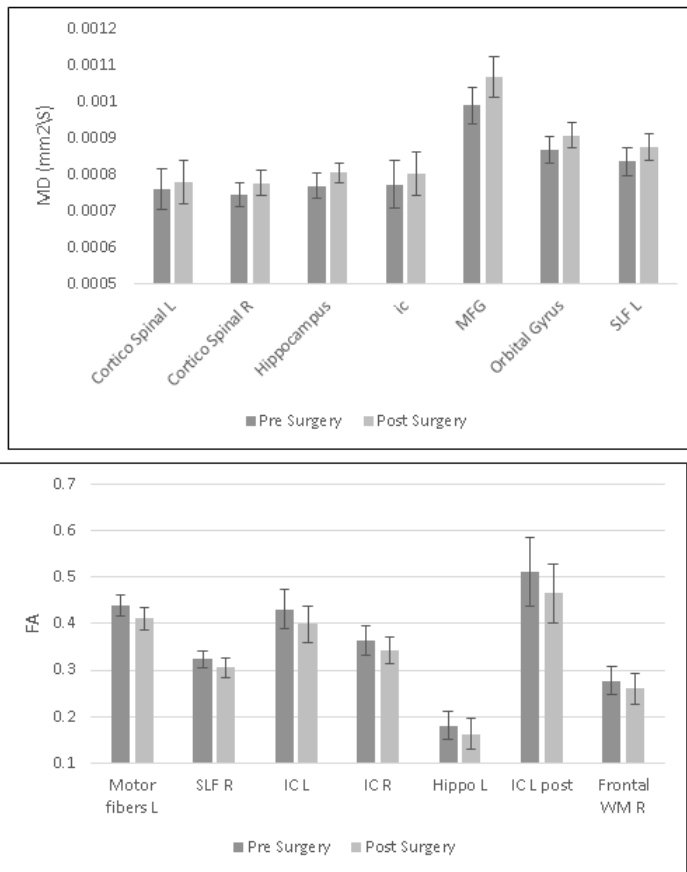


Figure 3: Voxel based paired T-test comparing mean MD and FA in gray and white matter structures – preoperative vs POD1.

Fibre tracing of the corticospinal tract showed significant postoperative decrease in fibre number (Figures 4 and 5).

These DTI findings persisted on POD 5 (Figures 6 and 7).

BBB disruption represented by an increase in the BBB permeability constant- K^{trans} was demonstrated in five patients (71%) on POD 1. Complete resolution was evident on POD 5 (Figure 8).

DWI signs of embolization were evident in only one patient (14%).

Postoperative global cognitive score was reduced in all patients (98.2 ± 12 versus 95.1 ± 11 , $p=0.032$), predominantly in executive function and attention (91.8 ± 13 versus 86.9 ± 12 , $p=0.042$) (Figure 9).

Postoperative FA decline significantly correlated with postoperative ΔK^{trans} . ($R=0.6$) (Figure 10) and with postoperative decline in attention and Go no Go response inhibition tests ($R=0.63$ and 0.66 respectively) (Figure 11).

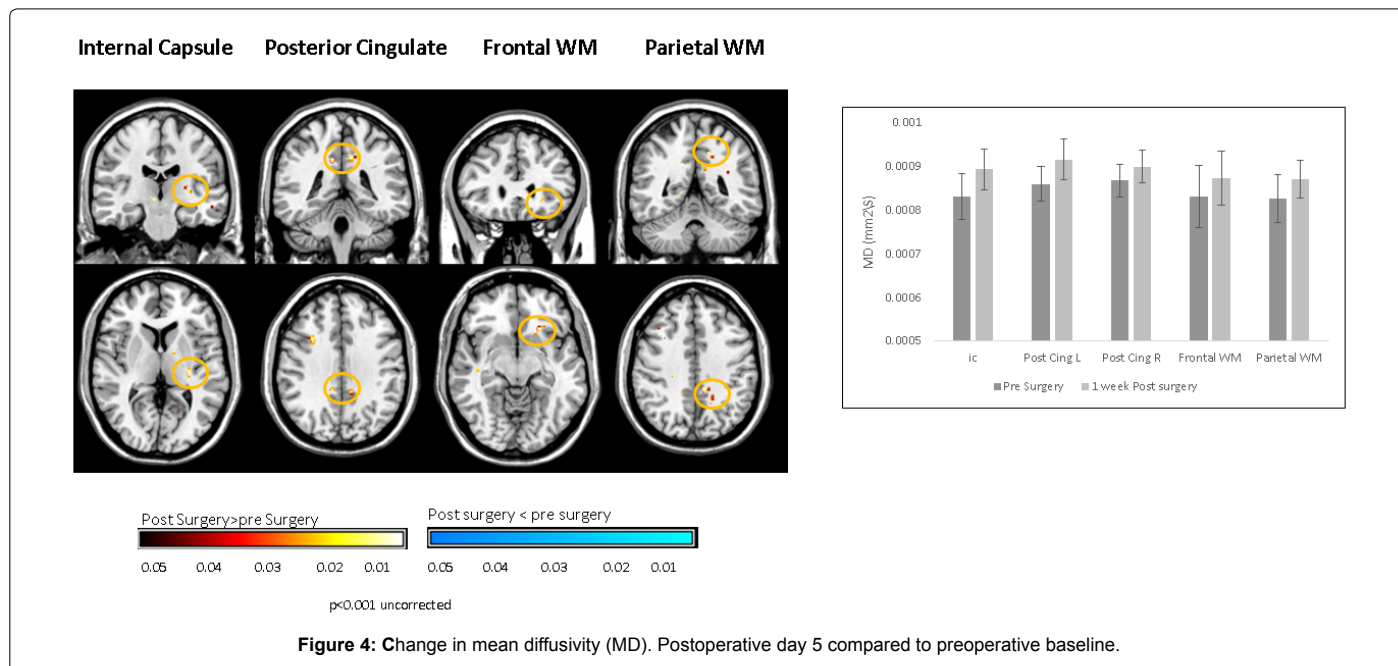


Figure 4: Change in mean diffusivity (MD). Postoperative day 5 compared to preoperative baseline.

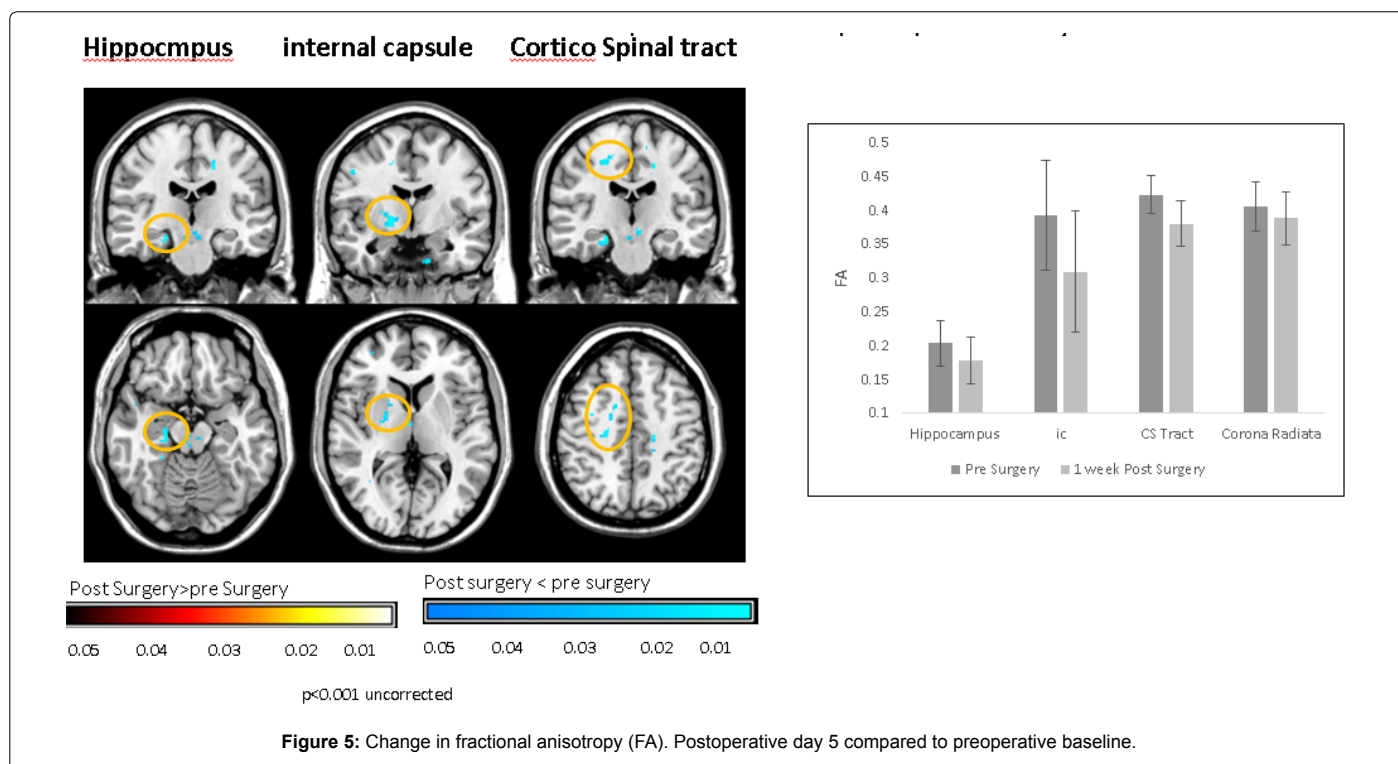


Figure 5: Change in fractional anisotropy (FA). Postoperative day 5 compared to preoperative baseline.

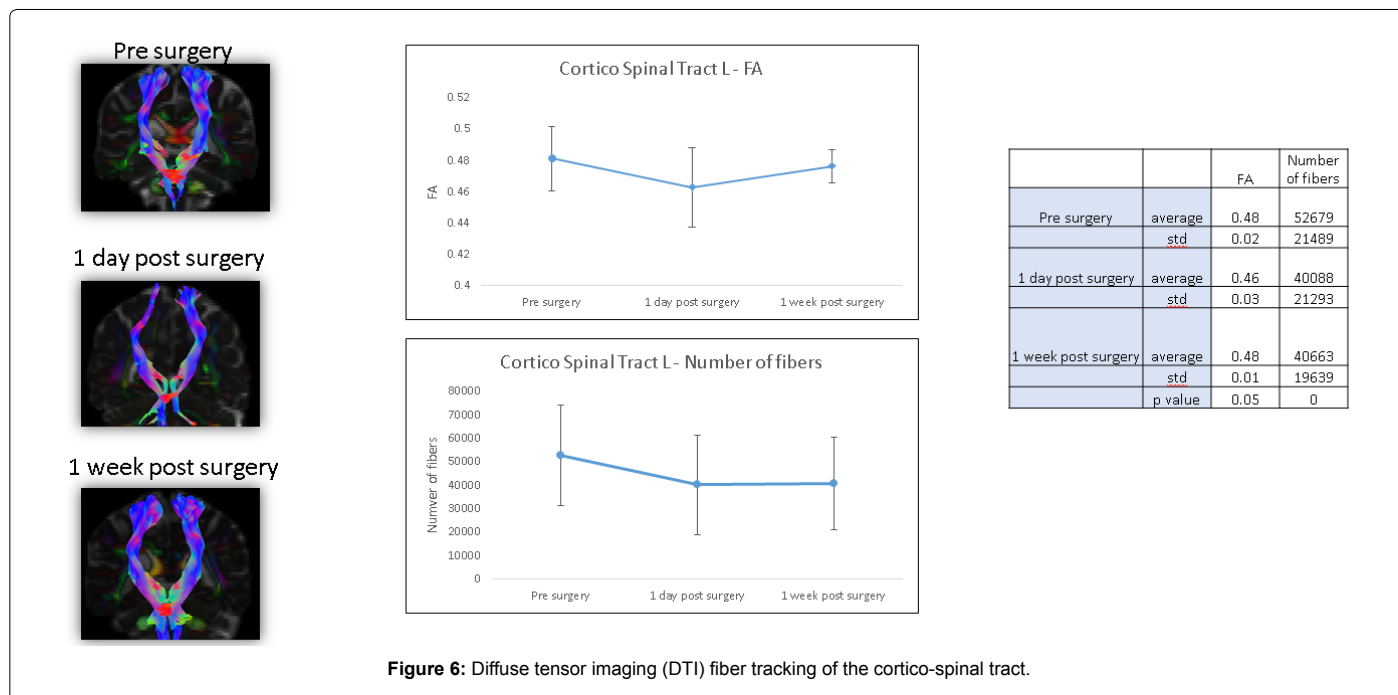


Figure 6: Diffuse tensor imaging (DTI) fiber tracking of the cortico-spinal tract.

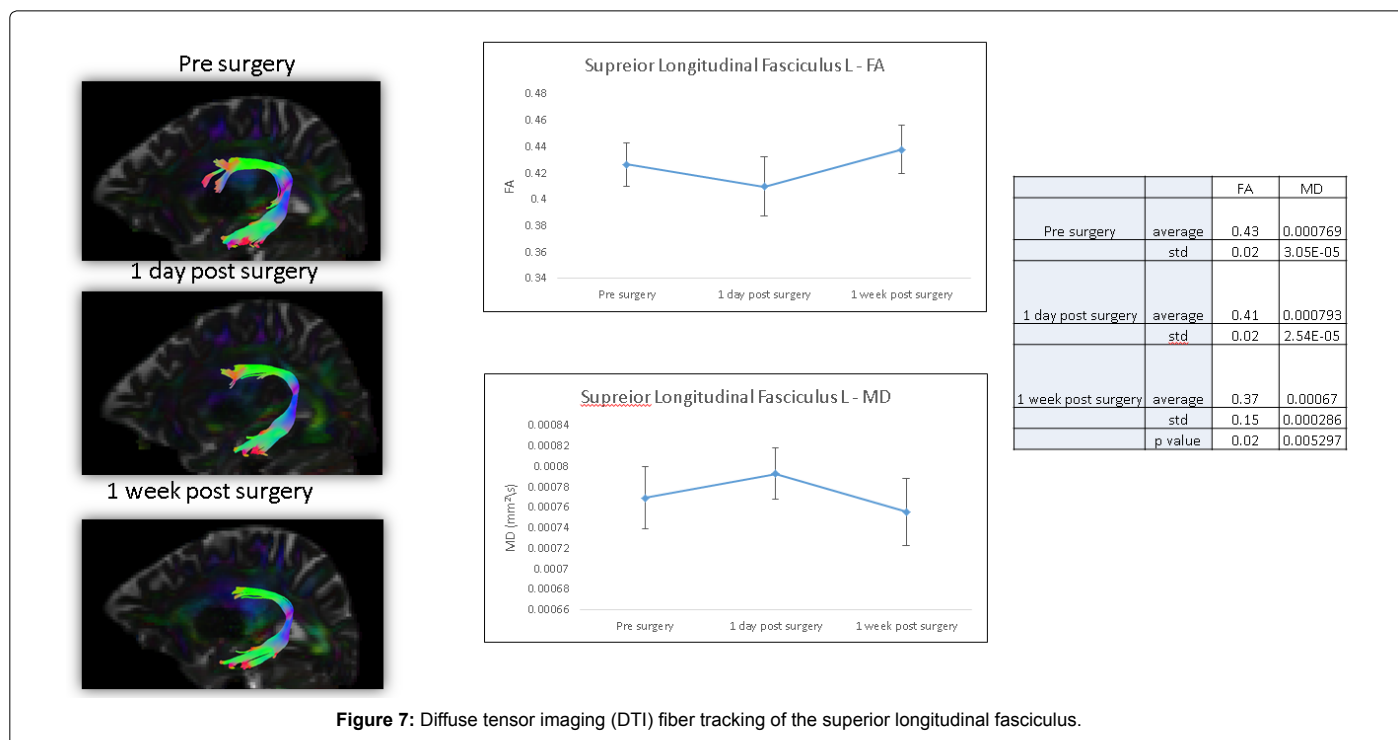


Figure 7: Diffuse tensor imaging (DTI) fiber tracking of the superior longitudinal fasciculus.

Discussion

The results of this study indicate that CABG using CPB is associated with microstructural brain injury in white and gray matter. Alterations were evident in white matter structures such as the superior longitudinal fasciculus, frontal white matter, internal capsule and corticospinal tract and in gray matter structures including the hippocampus, middle frontal gyrus and orbital gyrus. Specific fibre tracking has shown postoperative decrease in number of fibres in the corticospinal tract. Concomitant

self-limited BBB-disruption has been demonstrated and may account for these anatomical alterations. Considering neuroanatomical models and the statistical correlation with neuropsychological tests in this study, these anatomical alterations may account for the occurrence of postoperative neurocognitive dysfunction.

To date, available studies have failed to anatomically localize specific damaged zones in the brain that may explain the occurrence of neurocognitive dysfunction in patients that underwent otherwise

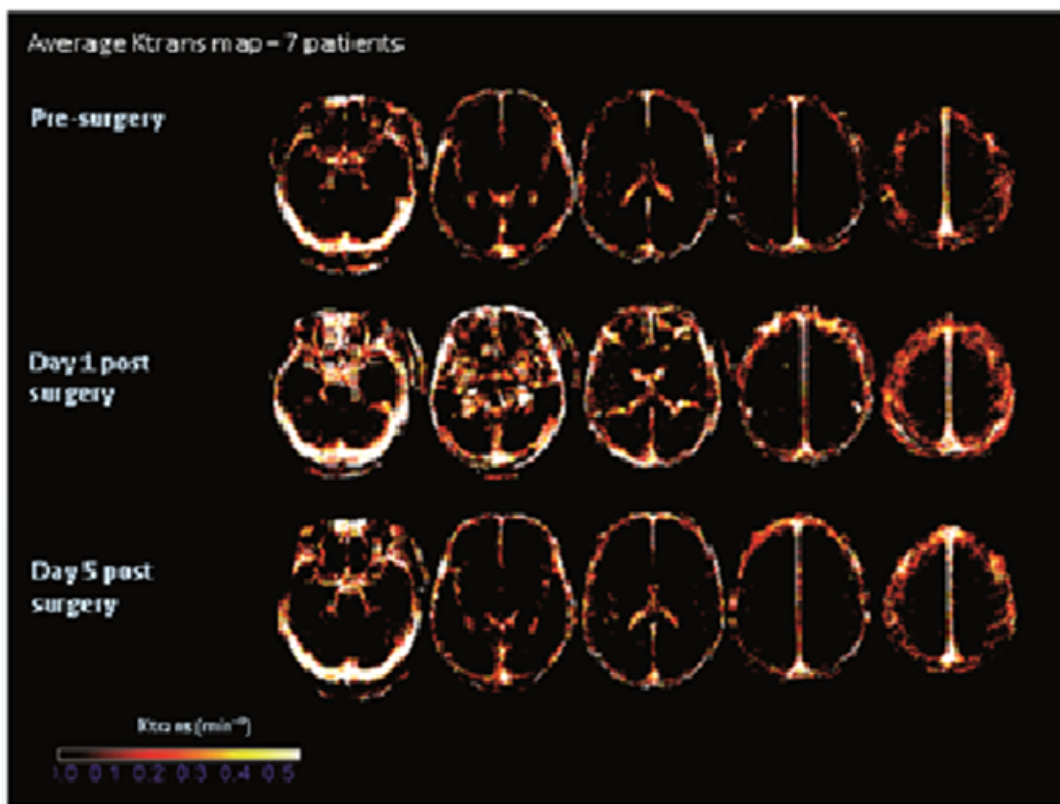


Figure 8: Average K^{trans} of 7 patients demonstrating BBB disruption. BBB-disruption is evident on POD 1 predominantly in the frontal area and restored on POD 5.

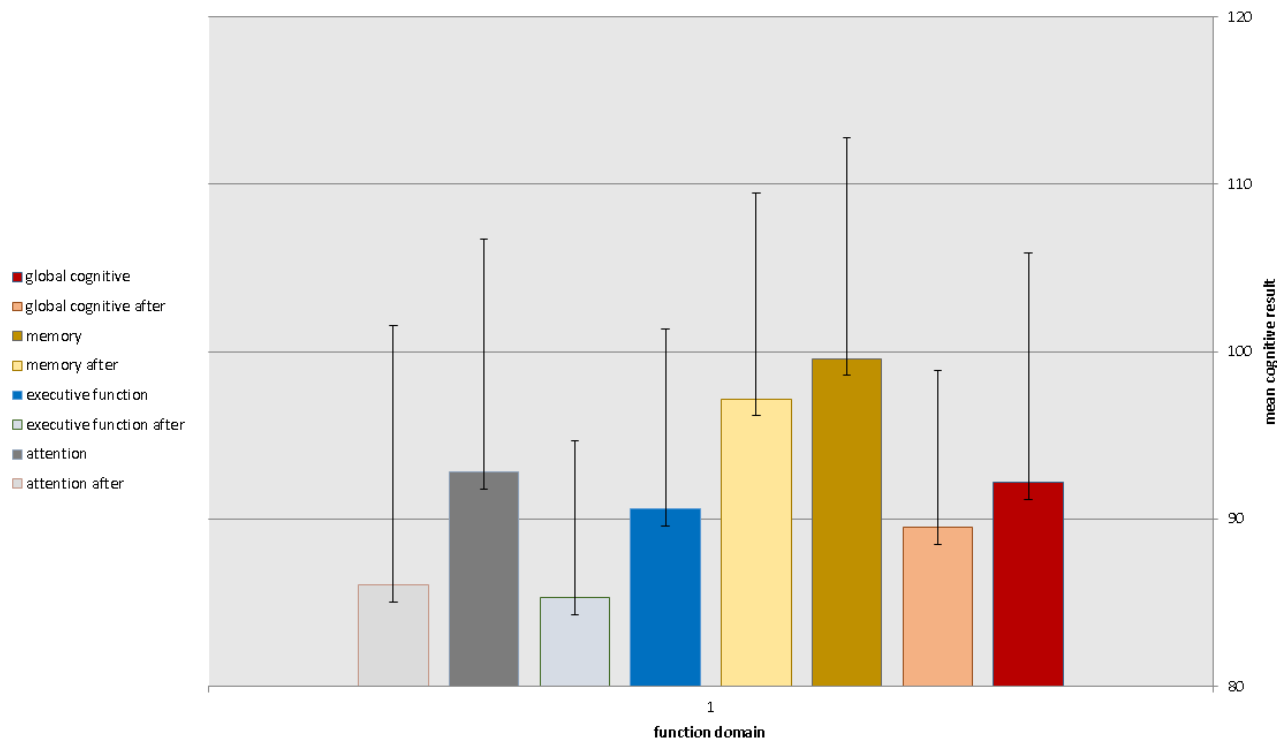


Figure 9: Neuropsychological test results before and after surgery.

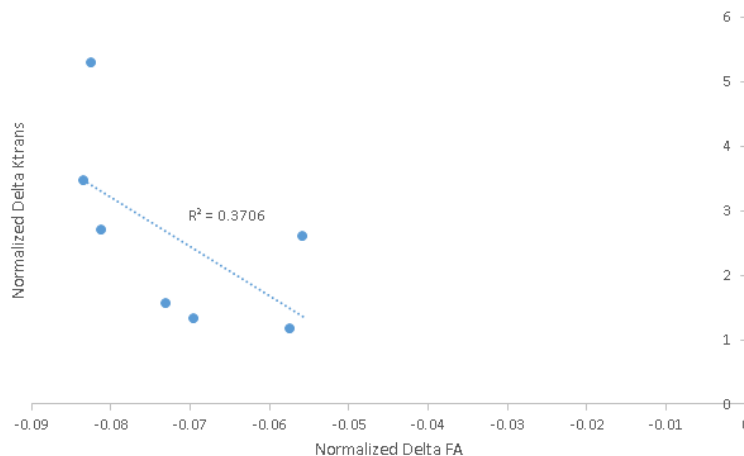


Figure 10: Correlation between average normalized delta fractional anisotropy (FA) and delta K^{trans} .

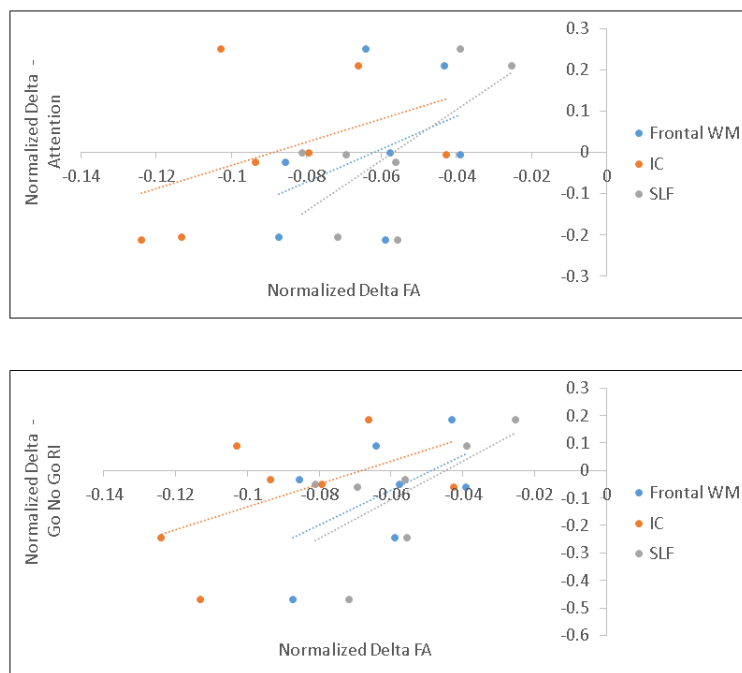


Figure 11: Correlation between normalized delta fractional anisotropy (FA) and postoperative change in Attention function. Correlation between normalized delta fractional anisotropy (FA) and postoperative change in Go no Go response inhibition test.

uneventful cardiac operations. Literature search has yielded 12 studies comprising of 446 patients that describe brain findings in the settings of cardiac surgery using standard MRI or DWI-MRI examinations [3,4,11-20]. The incidence of detected radiological lesions was 29% of patients usually interpreted as cerebral microembolism [11-20]. Nevertheless, the anatomical location of the newly evident lesions could not necessarily explain concomitant findings of postoperative neurocognitive deterioration based on recognized neuroanatomical models [12,13]. Also, correlation was not established between patients who displayed new radiological brain lesion and those who demonstrated postoperative neurocognitive dysfunction [11-20].

DTI is a recently developed MRI modality that provides information about the microstructure of both white and gray matter

and can portray a map of the brain neural tracts (tractography). Water molecules diffusion measured in six non-colinear directions is used to form a three dimensional representation of water motion and diffusion-patterns reveal details about microscopic tissue architecture [7,8].

Diffusion parameters calculated for each voxel are mean diffusivity (MD) and fractional anisotropy (FA), representing diffusion-average in all spatial directions and the difference between the largest diffusion vector and other vectors, respectively. Given that axons are in parallel bundles and lateral diffusion is hindered by myelin sheaths, water molecules-diffusion is normally directed along fibers' direction, represented by increased FA and decreased MD values. Conversely, damage to axons or myelin results in diffusion which is no longer

restricted to the axonal direction and overall diffusion increases reflected by decreased FA and increased MD [7, 8].

MRI-DTI is, therefore, particularly effective in disorders involving axonal damage or demyelination. It is used as an indicator of cerebral white matter integrity, to enhance small-scale tissue resolution and to differentiate between specific white matter tracts [21-24]. The yield of this technique has been previously validated in several settings. In mild traumatic brain injury and cerebral small vessel disease DTI metrics have yielded better prediction of cognitive function compared to lesion load demonstrated on T2 [22-24]. In patients with minimal cognitive impairment, hippocampal changes in MD and FA values and microstructural changes in the hippocampus had higher correlation with cognitive impairment compared to hippocampal volume measurements of standard MRI [24]. Noteworthy, increased MD and decreased FA values detected in the right and left entorhinal cortices, posterior occipital-parietal cortex, right parietal supramarginal gyrus and right frontal precentral gyrus correlated with deficits in neuropsychological measurements [24]. In Alzheimer's disease DTI studies have demonstrated significant reduction in frontal white matter integrity, undetected by standard MRI [22].

In this study voxel based paired DTI parameters were compared before and after surgery. The whole brain was measured using DTI. Regions with significant postoperative changes in the group analysis were highlighted (Figures 1-3). The changes were detected in high cognitive function-related gray matter structures (hippocampus, mediofrontal gyrus and orbital gyrus), high cognitive function-related white matter structures (superior longitudinal fasciculus, frontal white matter) and in motor related tracts (internal capsule and corticospinal tract).

The results of concomitant neuropsychological tests showed significant postoperative decrease in global cognitive function, in which the most prominent decrease was in attention and executive functions. Acknowledged neuroanatomical models of executive functions describe three circuits of cortical-subcortical structures, namely, the mediofrontal circuit, the orbitofrontal circuit and the dorsolateral prefrontal circuit [25], which are responsible for volition, behavior and executive functions, respectively. Correspondingly, the mediofrontal circuit is responsible for volition and consists of the anterior cingulate which connects to the ventromedial striatum, globus pallidus, substantia nigra and the mediodorsal thalamus which projects back to the anterior cingulate. The anterior cingulate has also connections with the dorsolateral prefrontal cortex (DLPFC). The orbitofrontal circuit is responsible for behavior and consists of the orbitofrontal cortex which connects to the ventromedial caudate nucleus, the globus pallidus and the dorsal thalamic nuclei. The orbitofrontal cortex also has interconnections with the DLPFC, the temporal pole and amygdala. The dorsolateral prefrontal circuit is responsible for executive functions and consists of the DLPFC which connects to the dorsolateral caudate nucleus, the lateral and dorsomedial globus pallidus and the ventral and mediodorsal thalamic nuclei.

Based on these neuroanatomical models, the sites of postoperative brain alterations demonstrated postoperatively in our cohort consistent with the cognitive deficits shown in the neuropsychological tests. Decreased FA values found in the anterior cingulate/cingulum and part of the ventromedial striatum which are both part of the mediofrontal circuit. Increased MD values found in the medial frontal gyrus and orbital gyrus, which are both part of the orbitofrontal circuit. Decreased FA values detected in frontal white matter (adjacent to the medial frontal gyrus) which is part of the dorsolateral prefrontal circuit.

Injuries in internal capsule and corticospinal motor tract correspond to a decline in Go no Go response inhibition by impeding the motor part of tasks.

In addition to the link between the distribution of neuroanatomical injury and executive functions, alteration in frontal white matter, internal capsule and superior longitudinal fasciculus reflected by decrease in FA may account for attention and Go no Go response inhibition decline. To our knowledge, such correlation between anatomical localization of brain injury and neuropsychological tests after CABG has not been previously documented.

In an attempt to explain postoperative neurocognitive deficits previous reports have mainly focused on traditional MRI signs of microemboli. Conversely, DWI-MRI analyses used in this study to detect brain microemboli have yielded postoperative signs of microemboli in only one patient (14%) and cannot explain the extent of the DTI-MRI findings or the extent of evident neurocognitive deficits.

Using DCE-MRI, BBB-disruption has been recently demonstrated after CABG using CPB [15,24]. Loss of BBB integrity was transient and resolved spontaneously within several days [15]. In DCE-MRI modality, BBB disruption is displayed as an increase in BBB permeability constant (K^{trans}) and enhancement kinetics can be used to extract quantitative information enabling to calculate K^{trans} for each voxel of the brain image [8]. In the present study a significant statistical correlation has been shown between postoperative ΔK^{trans} indicative of BBB disruption and decrease in FA values reflecting white matter injury. Although BBB-disruption was transient and restored spontaneously, the signs of white matter microstructure injury persisted throughout POD 5.

A mechanism for microstructural brain injury after CABG using CPB is, therefore, suggested. Inflammatory process, alone or in combination with microembolic and/or hypoperfusion events [1,2], elicits BBB-disruption and results in exposure of brain tissue to inflammatory substances, otherwise confined to the vasculature. These untoward substances account for microstructural brain tissue injury. As presented, there are specific brain regions which are more vulnerable to this type of insult. While BBB integrity is spontaneously regained within several days, brain tissue injury apparently persists, explaining the prolonged nature of the neurocognitive dysfunction.

Our study cohort was comprised of relatively uncomplicated, young patients, undergoing straightforward cardiac surgery. We therefore surmise that in the more complicated patients undergoing complex cardiac surgery, a more extensive brain injury is likely to ensue.

As post cardiac surgery survival has improved substantially in the past decades, emphasis should now be directed toward lowering postoperative sequels, neurocognitive deterioration being one of the most significant.

Study limitations

The power of this pilot study is limited by the small sample-size and subsequent statistical limitations. Neuropsychological studies including a scale to assess mood and affect involvement would have enhanced the validity of the anatomical findings. Also, it seems that non-invasive neurophysiological techniques investigating the functional integrity and connectivity of cortical-spinal tract, such as Transcranial Magnetic Stimulation (TMS) should be included in future studies.

The results of this study should further be scrutinized and corroborated in larger cohorts

To conclude, CABG using CPB is associated with microstructural

white matter injury in the distribution of the superior longitudinal fasciculus, frontal white matter, internal capsule and corticospinal tract and gray matter injury in the distribution of the hippocampus, middle frontal gyrus and orbital gyrus. These alterations are evident early after surgery and persist throughout POD 5. Whether these microstructural changes are permanent or eventually reversible remains undetermined and should be the focus of further study. The anatomical distribution of white and gray matter injury may explain the occurrence of postoperative neurocognitive dysfunction. Larger datasets are required to validate these observations.

References

1. Selnes OA, Goldsborough MA, Borowicz LM, McKhann GM (1999) Neurobehavioural sequelae of cardiopulmonary bypass. *Lancet* 353: 1601-1606.
2. Newman MF, Mathew JP, Grocott HP, Mackensen GB, Monk T, et al. (2006) Central nervous system injury associated with cardiac surgery. *Lancet* 368: 694-703.
3. Newman MF, Kirchner JL, Phillips-Bute B, Gaver V, Grocott H, et al. (2001) Longitudinal assessment of neurocognitive function after coronary artery bypass surgery. *N Engl J Med* 344: 395-402.
4. Aberg T, Ronquist G, Tydén H, Brunnkvist S, Bergström K (1987) Cerebral damage during open-heart surgery. Clinical, psychometric, biochemical and CT data. *Scand J Thorac Cardiovasc Surg* 21: 159-163.
5. Sotaniemi KA, Mononen H, Hokkanen TE (1986) Long-term cerebral outcome after open-heart surgery. A five-year neuropsychological follow-up study. *Stroke* 17: 410-416.
6. Abrahamov D, Levran O, Naparstek S, Refaeli Y, Kaptson S, et al. (2017) Blood-brain-barrier disruption after cardiopulmonary bypass: Diagnosis and correlation to cognition. *Ann Thorac Surg* 104: 161-169.
7. Alexander AL, Lee JE, Lazar M, Field AS (2007) Diffusion tensor imaging of the brain. *Neurotherapeutics* 4: 316-329.
8. Mukherjee P, Bermana JI, Chunga SW, Hessa CP, Henrya RG (2008) Diffusion tensor MR imaging and fiber tractography: Theoretic underpinnings. *AJNR Am J Neuroradiol* 29: 632-641.
9. Wessels T, Röttger C, Jauss M, Kaps M, Traupe H, et al. (2005) Identification of embolic stroke patterns by diffusion-weighted MRI in clinically defined lacunar stroke syndromes. *Stroke* 36: 757-761.
10. Heye ak, Culling RD, Hernández MV, Thrippleton MJ, Wardlaw JM (2014) Assessment of blood brain barrier disruption using dynamic contrast enhanced MRI. A systemic review. *Neuroimage Clin* 6: 262-274.
11. Bendszus M, Reents W, Franke D, Müllges W, Babin-Ebell J, et al. (2002) Brain damage after coronary bypass grafting. *Arch Neurol* 59: 1090-1095.
12. Restrepo L, Wityk RJ, Grega MA, Borowicz L Jr, Barker PB, et al. (2002) Diffusion- and perfusion-weighted magnetic resonance imaging of the brain before and after coronary artery bypass grafting surgery. *Stroke* 33: 2909-2915.
13. Knipp SC, Matatko N, Wilhelm H, Schlamann M, Massoudy P, et al. (2004) Evaluation of brain injury after coronary artery bypass grafting: A prospective study using neurological assessment and diffusion-weighted magnetic resonance imaging. *Eur J Cardiovasc Surg* 25: 791-800.
14. Djaiani G, Fedorko L, Borger M, Mikulis D, Carroll J, et al. (2004) Mild to moderate atheromatous disease of the thoracic aorta and new ischemic brain lesions after conventional coronary artery bypass graft surgery. *Stroke* 35: e356-e358.
15. Gerriets Stolz E, Kluge A, Klövekorn WP, Kaps M, Bachmann G (2004) Diffusion-weighted magnetic resonance imaging and neurobiochemical markers after aortic valve replacement: Implications for future neuroprotective trials? *Stroke* 35: 888-892.
16. Knipp SC, Matatko N, Schlamann M, Wilhelm H, Thielmann M, et al. (2005) Small ischemic brain lesions after cardiac valve replacement detected by diffusion-weighted magnetic resonance imaging: Relation to neurocognitive function. *Eur J Cardiovasc Surg* 28: 88-96.
17. Friday G, Sutter F, Curtin A, Kenton E, Caplan B, et al. (2005) Brain magnetic resonance imaging abnormalities following off-pump cardiac surgery. *Heart Surg Forum* 8: E105-E109.
18. Floyd TF, Shah PN, Price CC, Harris F, Ratcliffe SJ, et al. (2006) Clinically silent cerebral ischemic events after cardiac surgery: their incidence, regional vascular occurrence and procedural dependence. *Ann Thorac Surg* 81: 2160-2166.
19. Djaiani G, Fedorko L, Cusimano RJ, Mikulis D, Carroll J, et al. (2006) Off-pump coronary bypass surgery: Risk of ischemic brain lesions in patients with atheromatous thoracic aorta. *Can J Anesth* 53: 795-801.
20. Cook DJ, Huston J, Trenerry MR, Brown R, Zehr KJ, et al. (2007) Postcardiac surgical cognitive impairment in the aged using diffusion-weighted magnetic resonance imaging. *Ann Thorac Surg* 83: 1389-1395.
21. Niogi SN, Mukherjee P (2010) Diffusion tensor imaging of mild traumatic brain injury. *J Head Trauma Rehabil* 25: 241-255.
22. van Norden AG, de Laat KF, van Dijk EJ, van Uden IW, van Oudheusden LJ, et al. (2012) Diffusion tensor imaging and cognition in cerebral small vessel disease: The RUN DMC study. *Biochim Biophys Acta* 1822: 401-407.
23. Stebbins GT, Murphy CM (2009) Diffusion tensor imaging in Alzheimer's disease and mild cognitive impairment. *Behav Neurol* 21: 39-49.
24. Rose SE, McMahon KL, Janke AL, O'Dowd B, de Zubicaray G, et al. (2006) Diffusion indices on magnetic resonance imaging and neuropsychological performance in amnesic mild cognitive impairment. *J Neurol Neurosurg Psychiatry* 77: 1122-1128.
25. Gunning-Dixon FM, Raz N (2003) Neuroanatomical correlates of selected executive functions in middle-aged and older adults: A prospective MRI study. *Neuropsychologia* 41: 1929-1941.